

Adaxial/abaxial specification in the regulation of photosynthesis and stomatal opening with respect to light orientation and growth with CO₂ enrichment in the C₄ species *Paspalum dilatatum*

Ana Sofia Soares^{1,2}, Simon P. Driscoll¹, Enrique Olmos³, Jeremy Harbinson⁴, Maria Celeste Arrabaça² and Christine H. Foyer^{1,5}

¹Crop Performance and Improvement Division, Rothamsted Research, Harpenden, Hertfordshire AL5 2JQ, UK; ²Centro de Engenharia Biológica & Departamento de Biologia Vegetal, Faculdade de Ciências da Universidade de Lisboa, Campo Grande 1749-016 Lisboa, Portugal; ³CEBAS-CSIC, Department of Plant Physiology, PO Box 164, 30080-Murcia, Campus de Espinardo, Spain; ⁴Wageningen University, Department of Plant Sciences, Horticultural Production Chains Group, Marijkeweg 22, 6709 PG Wageningen, the Netherlands; ⁵Present address: School of Agriculture, Food and Rural Development, Agriculture Building, The University of Newcastle upon Tyne, Newcastle upon Tyne NE1 7RU, UK

Summary

Author for correspondence:

Christine H. Foyer

Tel: +44 1912226932

Fax: +44 1912227811

Email: christine.foyer@newcastle.ac.uk

Received: 17 June 2007

Accepted: 23 July 2007

- Whole-plant morphology, leaf structure and composition were studied together with the effects of light orientation on the dorso-ventral regulation of photosynthesis and stomatal conductance in *Paspalum dilatatum* cv. Raki plants grown for 6 wk at either 350 or 700 µl l⁻¹ CO₂.
- Plant biomass was doubled as a result of growth at high CO₂ and the shoot:root ratio was decreased. Stomatal density was increased in the leaves of the high CO₂-grown plants, which had greater numbers of smaller stomata and more epidermal cells on the abaxial surface.
- An asymmetric surface-specific regulation of photosynthesis and stomatal conductance was observed with respect to light orientation. This was not caused by dorso-ventral variations in leaf structure, the distribution of phosphoenolpyruvate carboxylase (PEPC) and ribulose 1,5-bisphosphate carboxylase/oxygenase (Rubisco) proteins or light absorbance, transmittance or reflectance.
- Adaxial/abaxial specification in the regulation of photosynthesis results from differential sensitivity of stomatal opening to light orientation and fixed gradients of enzyme activation across the leaf.

Key words: abaxial/adaxial leaf specification, CO₂ enrichment, phosphoenolpyruvate carboxylase (PEPC), photosynthesis, ribulose 1,5-bisphosphate carboxylase/oxygenase (Rubisco), stomatal patterning.

New Phytologist (2008) **177**: 186–198

© The Authors (2007). Journal compilation © *New Phytologist* (2007)

doi: 10.1111/j.1469-8137.2007.02218.x

Introduction

Photosynthesis plays a crucial role in ecosystem sustainability (Millennium Ecosystem Assessment, 2005). In order to combat climate change and ensure the sustainability of natural and cultivated ecosystems, it is essential to understand

the responses of photosynthesis to fluctuating environmental conditions, particularly atmospheric CO₂ enrichment. Surprisingly little attention has been given to the effects of increased atmospheric CO₂ on C₄ photosynthesis, despite the fact that many of the most productive bio-energy/bio-fuel crops are monocotyledonous C₄ species. It is important,

therefore, to gain a better understanding of how CO₂ enrichment will alter stomatal function and photosynthesis in such species, and particularly to elucidate any interactions with respect to light orientation, which is a crucial regulator of these processes (Poulson & DeLucia, 1993). Structure–function relationships in photosynthesis have been intensely studied in dicotyledonous leaves (Terashima & Saeki, 1983; Cui *et al.*, 1991; Vogelmann, 1993), which exhibit internal gradients in light and photosynthetic capacity (Terashima & Inoue, 1985a,b). The highest photosynthesis rates are not found near the leaf surface where the light intensity is highest, but are observed in the middle and lower palisade layers (Nishio *et al.*, 1993; Evans, 1995; Sun *et al.*, 1998; Sun & Nishio, 2001; Evans & Vogelmann, 2003), which have higher electron transport activities and greater amounts of photosynthetic proteins (Terashima & Inoue, 1985b; Terashima & Evans, 1988; Sun & Nishio, 2001). The adaxial surfaces of dicotyledonous C₃ leaves have characteristics that resemble classic ‘sun’ leaves, while the abaxial surfaces have properties that are consistent with ‘shade’ leaves (Oya & Laisk, 1976; Terashima, 1986; Terashima & Evans, 1988; Lambers *et al.*, 1998). Growth at high CO₂ alters the regulation of photosynthesis on the adaxial and abaxial leaf surfaces of maize (*Zea mays*) leaves (Domes, 1971; Driscoll *et al.*, 2006), but very little information is available on the effects of CO₂ enrichment on the surface-specific regulation of photosynthesis in other monocotyledonous C₄ species.

Atmospheric CO₂ availability exerts a strong influence on the dorso-ventral organization of leaf structure, composition and photosynthetic activity (Taylor *et al.*, 1994, 2001; Croxdale, 1998; Masle, 2000; Lake *et al.*, 2001; Poorter & Navas, 2003; Martin & Glover, 2007). Similarly, growth CO₂ concentrations exert control over stomatal density and patterning (Larkin *et al.*, 1997; Lake *et al.*, 2002). Atmospheric CO₂ enrichment decreases stomatal densities in the leaves of dicotyledonous C₃ species (Woodward *et al.*, 2002). However, the degree of this response to CO₂ enrichment differs between species and little information is available in the literature on such effects in monocotyledonous C₄ species (Woodward & Kelly, 1995; Woodward *et al.*, 2002). The CO₂-signalling pathways that orchestrate these changes in leaf structure and composition responses remain poorly characterized (Gray *et al.*, 2000; Ferris *et al.*, 2002), but signals transported from mature to developing leaves are considered to be important regulators of such responses (Coupe *et al.*, 2006; Miyazawa *et al.*, 2006).

The present study was undertaken in order to characterize the relative effects of light orientation and CO₂ availability on photosynthesis and stomatal responses in *Paspalum dilatatum*, which, like maize, is a C₄ monocotyledonous species of the NADP-malic enzyme (NADP-ME) subtype. *Paspalum dilatatum* is a common grass species of the prairies of South America (Pinto da Silva, 1969; Usuda *et al.*, 1984) and the wetter areas of Australia (Pearson *et al.*, 1985; Brown, 1999) and has already been characterized in terms of photosynthetic

responses to environmental stress (e.g. Marques da Silva *et al.*, 1991; Bernardes da Silva *et al.*, 1999; Cavaco *et al.*, 2003; Carmo-Silva *et al.*, 2007) and to CO₂ enrichment (Greer *et al.*, 1995; von Caemmerer *et al.*, 2001). Here we report the influence of light orientation on the dorso-ventral regulation of photosynthesis and stomatal conductance, and the effect of growth CO₂ on the symmetry of the photosynthetic responses on the adaxial and abaxial leaf surfaces to incident light (either adaxial or abaxial), together with acclimatory responses in whole-plant morphology, biomass, whole-leaf photosynthesis, stomatal patterning and leaf composition.

Materials and Methods

All the following experiments were conducted in the laboratories at Rothamsted Research, Harpenden, UK except for the electron microscopy, which was performed at CEBAS-CSIC, Murcia, Spain on samples prepared at Rothamsted Research. Each experiment was repeated at least three times and all experiments involved a minimum of three plants.

Seeds of *Paspalum dilatatum* Poir. cv. Raki were obtained from the Margot Forage Germplasm Centre, Palmerston North, New Zealand. They were germinated on compost containing slow-release fertilizer in pots (20 cm diameter) and then grown for 6 wk in two controlled-environment cabinets (Sanyo SGC228.CFX.J; Sanyo, Osaka, Japan) in which all the growth conditions were identical except for the atmospheric CO₂ concentration, which was maintained at either 350 or 700 µl l⁻¹ throughout the duration of the experiments. CO₂ was supplied from a bulk container via a Vaisala GMT220 CO₂ transmitter (Vaisala Oyj, Helsinki, Finland). The CO₂ contents within the chambers were maintained at 350 ± 20 or 700 ± 20 µl l⁻¹ using a Eurotherm 2704 controller (Eurotherm Ltd, Worthing, UK). The plants were grown under a 16-h photoperiod with a 25°C (day): 19°C (night) temperature regime and 80% relative humidity. Irradiance (600–650 nmol µmol m⁻² s⁻¹ at 400–700 nm, at pot height) was provided by Philips Master TL5 HO 49w/830 fluorescent lamps (Philips Lighting UK, Guildford, UK). All plants were well watered daily and the root growth in the pots was checked periodically to ensure that an appropriate pot size was used throughout the growth period. At the harvest point the roots were growing freely.

Whole-plant growth parameters and tissue biomass

In each experiment, between eight and 14 plants were harvested at 6 wk from each CO₂ chamber, a time-point that was before anthesis in both air- and high CO₂-grown plants. Harvested plants were separated into leaves, stems and roots. The following measurements were performed: root, stem and leaf biomass, specific leaf area (SLA), leaf area ratio (LAR), leaf weight ratio (LWR), leaf density (% leaf dry weight (DW)) and leaf thickness (leaf fresh weight to leaf area ratio).

Photosynthesis measurements

Photosynthetic gas-exchange measurements were performed using infrared gas analysis (model wa-225-mk3; ADC, Hoddesdon, UK). Two different types of chamber system were used in these studies. One apparatus involves a series of standard Parkinson chambers for whole-leaf measurements (Novitskaya *et al.*, 2002). The second apparatus uses modified Parkinson chambers, as illustrated in Fig. 1. This system enables separate and simultaneous measurements of gas exchange on each leaf surface (Driscoll *et al.*, 2006).

To check the degree of CO₂ transport across the leaf, a gas stream containing 10% CO₂ was applied to each surface independently in the chamber and the concentration on the other surface was measured. In this system, we could detect no passage of CO₂ from one surface to the other through the leaf blade. While the stomata close under these conditions, this simple experiment illustrates that there is no passage of gases from one side of the chamber to the other. Each half of this dual chamber operates essentially as a whole leaf chamber as each half has a distinct gas supply and analysis unit with separate humidity, leaf temperature and individual fan controls (Fig. 1a,b,c). Flow rates were optimized on each side of the chamber to match the pressure on both leaf surfaces. Because the *P. dilatatum* leaf was not large enough to fully separate the two sides of the chamber, the leaf was expanded with gas-tight tape to seal each half of the chamber, preventing any flux of gas between the two sides (Fig. 1d,e). Irradiance was supplied only from the top of the chamber as described previously (Novitskaya *et al.*, 2002). Leaf temperatures were monitored via thermocouples attached to each surface

separately (Fig. 1b) and were maintained by water jackets at 20°C on both the adaxial and abaxial surfaces to ensure that the illuminated surface had exactly the same temperature as the unilluminated surface. All experiments were conducted at 50% relative humidity. The gas composition was controlled by gas mixers supplying CO₂ at concentrations as indicated in the figures with 21% O₂ and balance N₂.

Attached last fully expanded leaves of the primary tiller of air- and CO₂-grown plants were used to obtain CO₂- and light-response curves for whole-leaf photosynthesis and photosynthesis on each leaf surface separately. Light was oriented directly to the adaxial surface or to the abaxial surface (by inverting the leaf in the chamber). For CO₂-response curves, CO₂ was increased step-wise from 50 to 1000 µl l⁻¹ at an irradiance of between 900 and 1000 µmol m⁻² s⁻¹. Light-response curves for photosynthesis were obtained via step-wise increases in irradiance from darkness to 1500 µmol m⁻² s⁻¹ at 360 µl l⁻¹ CO₂. Steady-state gas-exchange measurements were obtained for each treatment after at least 10 min of incubation in each light and CO₂ condition. Vapour water deficit was kept constant throughout the assay in both types of analysis.

Leaf optical properties

Leaf reflectance and transmittance measurements were performed on each surface of *P. dilatatum* plants grown at 350 µl l⁻¹. Attached leaves of the same age and stage of development as those used for gas exchange were measured across the spectrum from 400 to 800 nm at 1-nm intervals. Five measurements were made on both sides of each leaf parallel to the middle vein and three leaves were assayed per

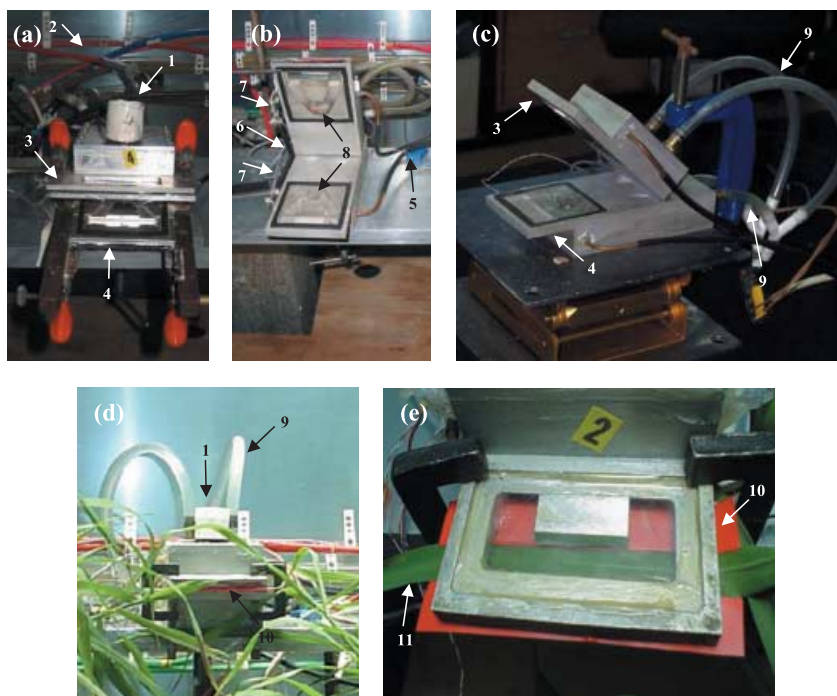


Fig. 1 The modified Parkinson leaf chamber used for separate and simultaneous gas exchange measurements on each leaf surface. Different views of the chamber are given to illustrate the following features: 1, light sensor; 2, connecting tubes to the infrared gas analyser; 3, upper side of the modified chamber with light source; 4, lower side of the modified chamber; 5, air supply in to both sides of the chamber; 6, air supply out of both sides of the chamber; 7, humidity and temperature sensors on both sides of the chamber; 8, fan on both sides of the chamber; 9, water jackets on both sides of the chamber; 10, gas-tight tape; 11, *Paspalum dilatatum* leaf.

experiment. Reflectance and transmittance were measured using reflection and irradiance integration spheres (Avasphere-30 reflection and irradiance integration spheres; Avantes, Eerbeek, the Netherlands) connected to a USB-2000 spectroradiometer (Ocean Optics, Dunedin, FL, USA). The measuring light was provided by a laboratory-built stabilized quartz-halogen source connected to a 0.6-mm optical fibre (type QP600-2-VIS-BX; Ocean Optics). In both cases the angle of incidence of the measuring beam was 8°. The 100% reflectance signal was obtained using a white reflectance standard (Spectralon; Labsphere, North Sutton, NH, USA). This was calibrated against a sheet of glass microfibre paper (Type GF/A; Whatman, Brentford, UK), which was used as a second standard. Leaf absorbance was calculated for each wavelength, as $1 - (\text{reflectance} + \text{transmittance})$.

Determination of pigments and protein content

Leaf pigments (chlorophyll *a* (chl*a*), chl*b*, total chlorophyll and carotenoids) and soluble protein contents were determined in the leaves of air- and high CO₂-grown plants. Leaf sections (4 cm), excised from both sides of each leaf parallel to the middle vein, were ground in liquid nitrogen and quartz sand. Pigments were determined according to the method of Lichtenhaler & Wellburn (1983) in ethanol (96%) extracts. Total leaf soluble proteins were extracted in 1 mM sodium phosphate buffer (pH 7.0) containing 10 mM dithiothreitol (DTT), 1 mM phenylmethanesulphonylfluoride or phenylmethylsulphonyl fluoride (PMSF), 5 mM 2-mercaptoethanol and 1% (weight/volume (w/v)) Polyclar AT (Sigma-Aldrich, Saint Louis, MO, USA). Protein was determined according to the method of Bradford (1976).

Analysis of epidermal structure

The structure of the epidermis was examined in the leaves of air- and high CO₂-grown plants using comparable sections to those used for photosynthesis measurements. Leaf sections were painted on the adaxial and abaxial surfaces with clear nail varnish. Epidermal imprints were then stripped from both surfaces and examined by optical microscopy (Olympus BH-2; Olympus Optical Co. Ltd, Tokyo, Japan). The number of stomata was counted on 24 randomly selected digitized images from the adaxial or the abaxial epidermal imprints of eight plants. To calculate epidermal and stomatal cell areas and densities, the dimensions of at least 100 cells from the adaxial or the abaxial epidermal layers were measured per experiment using SIGMA SCANPRO photographic analysis software, version 5 (Sigma Chemical Co., St Louis, MO, USA). The stomatal index was calculated as the number of stomata/(number of epidermal cells + number of stomata) × 100, as defined by Salisbury (1927). The ratio of stomata on each surface was calculated from the number of stomata counted on the adaxial and abaxial surfaces.

Fixation, embedding and sectioning for optical and electron microscopy

Leaf blade samples (1 mm²) were sectioned from the middle of the last fully expanded leaf of *P. dilatatum* plants grown at 350 µl l⁻¹ CO₂. Sections were fixed at ambient temperature in 4% (v/v) paraformaldehyde and 1% (v/v) glutaraldehyde in 0.2 M sodium phosphate buffer (pH 7.2) for 3.5 h. The samples were then washed in the same buffer three times for 15 min. They were then dehydrated at ambient temperatures using a graded ethanol series (35, 50, 70, 96 and twice at 100% (v/v) ethanol) with 30 min exposure at each step. The embedding was carried out in London Resin White acrylic resin (LRWhite; Electron Microscopy Sciences, Fort Washington, PA, USA) according to the following schedule: 75% (v/v) ethanol + 25% (v/v) LRWhite, 50% (v/v) ethanol + 50% (v/v) LRWhite, 25% (v/v) ethanol + 75% (v/v) LRWhite, 100% (v/v) LRWhite (1 h each series), and 100% (v/v) LRWhite overnight. The samples were transferred to tubes filled with resin and polymerized under nitrogen ambient at 55°C for 24 h. Transverse semithin leaf sections (0.5 µm) for optical microscopy and transverse ultrathin leaf sections for electron microscopy (50–60 nm) were prepared using a Leica EM UC6 ultramicrotome (Leica Microsystems, Wetzlar, Germany). Optical microscopy sections were stained with toluidine blue. Electron microscopy sections were mounted on nickel grids and stained with lead citrate (Reynolds, 1963) and 2% (w/v) uranyl acetate. Optical microscopy sections were observed using a Leica DMR light microscopy (Leica Microsystems, Wetzlar, Germany).

In situ immunolocalization of ribulose 1,5-bisphosphate carboxylase/oxygenase and phosphoenolpyruvate carboxylase

The nickel grids were incubated at ambient temperature for 30 min in phosphate-buffered saline (PBS) containing 5% (w/v) bovine serum albumin (BSA). They were then incubated at room temperature for 3 h with either rabbit preimmune serum (dilution 1 : 500), rabbit anti-ribulose 1,5-bisphosphate carboxylase/oxygenase (Rubisco) large subunit (Agrisera AB, Vännäs, Sweden) (dilution 1 : 250) or rabbit anti-phosphoenolpyruvate carboxylase (PEPC) (courtesy of Jean Vidal, Institut de Biotechnologie des Plantes, Centre National de la Recherche Scientifique, Université de Paris-Sud, France) (dilution 1 : 500), in the above PBS/BSA mixture. After washing twice with PBS (5 min each wash), the sections were incubated at ambient temperature for 1.5 h with goat anti-rabbit antibodies labelled with gold 10 nm (British Biocell International, Cardiff, UK) diluted in PBS containing 1% (w/v) BSA (dilution 1 : 50). The sections were washed sequentially with PBS containing 1% (w/v) BSA and then twice with PBS alone followed by five washes with filtered (0.2 µm) ultra-pure water (5 min each wash). The grids were

dried at ambient temperature. Immunogold electron microscopy images were collected using a Philips Tecnai 12 electron microscope (Philips, The Hague, the Netherlands) operated at 80 kV. The number of gold particles on the adaxial and abaxial sides of the leaves and the parameters of ultrastructural morphology were quantified using the 3.2 image analysis software (Soft Imaging System, Münster, Germany). Quantification of gold labelling was performed on three leaf samples per experiment with a total of 45 different bundle sheath (BS) and mesophyll (M) cells measured in each analysis.

Statistical analysis

The data were statistically analysed using parametric tests at a stringency of $P < 0.05$. The significance of variation in mean values for growth parameters and pigment and protein determinations was determined using a t -test. The significance of the data for epidermal structure and immunological measurements was analysed using ANOVA and Tukey HSD tests.

Results

Plant phenotype, leaf protein and pigment contents

Plants grown at the higher CO_2 concentration were larger with greater numbers of larger leaves than those grown at $350 \mu\text{l l}^{-1} \text{CO}_2$ (Fig. 2a, Table 1a). While plants grown at $700 \mu\text{l l}^{-1} \text{CO}_2$ had a higher shoot and root biomass, CO_2 enrichment decreased the shoot to root ratio (Table 1a). In contrast to the increase in leaf thickness, the SLA, LAR, LWR and leaf density values were not affected by doubling the growth CO_2 concentration (Table 1b). The leaf soluble protein contents were similar in the two growth conditions, but the high CO_2 -grown leaves generally had a slightly lower pigment content with less total carotenoids (7%) and chlorophyll (11%; Table 2).

Leaf epidermal structure

The epidermal cells on the adaxial leaf surface were arranged in parallel rows with stomata in every third or fourth row (Fig. 2b(i,iii)). In contrast, while the epidermal cells on the abaxial surface were similarly arranged in parallel rows, the stomata were located in every second or third row (Fig. 2b(ii,iv)). Moreover, the average stomatal area on the abaxial surface was lower than on the adaxial surface (Table 3). The average epidermal cell area was comparable on both leaf surfaces whether plants were grown at 350 or $700 \mu\text{l l}^{-1} \text{CO}_2$ (Table 3). The ratio of stomata on the adaxial compared with the abaxial surface was $c. 0.7$ at both growth CO_2 conditions (Fig. 2b, Table 3). However, the stomata were smaller in size and greater in number in plants grown at the high CO_2 concentration (Table 3). The lowest stomatal density was observed on the adaxial surface of leaves grown at $350 \mu\text{l l}^{-1} \text{CO}_2$ while the

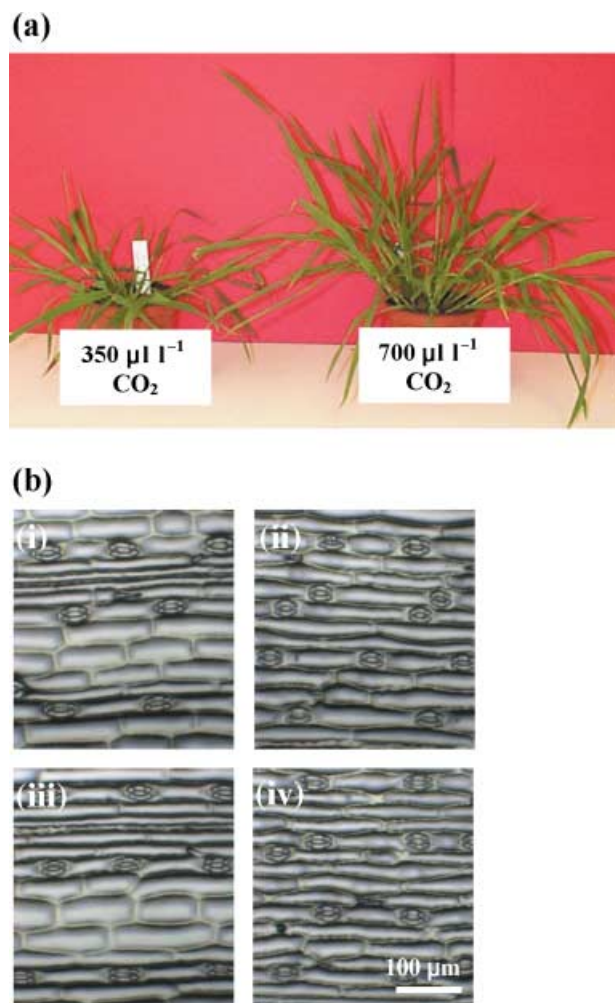


Fig. 2 A comparison of the effects of growth with CO_2 enrichment on *Paspalum dilatatum* (a) shoots and (b) leaf epidermal structure. Stomata and epidermal cells on the adaxial (i, iii) and abaxial leaf epidermis (ii, iv) of plants grown for 6 wk at either (i, ii) $350 \mu\text{l l}^{-1}$ or (iii, iv) $700 \mu\text{l l}^{-1} \text{CO}_2$ are shown. Bar, $100 \mu\text{m}$.

highest stomatal density was found on the abaxial surface of leaves grown at $700 \mu\text{l l}^{-1} \text{CO}_2$ (Table 3).

Whole-leaf photosynthesis, absorptance, transmittance and reflectance

Photosynthetic CO_2 assimilation rates increased as atmospheric CO_2 was increased over a range of low intercellular CO_2 concentrations (C_i), in a similar manner regardless of the growth CO_2 environment or light orientation (Fig. 3a(i,ii)). However, maximal steady-state rates of photosynthesis were slightly higher in air-grown plants when light was oriented to the adaxial surface (Fig. 3a(i)). The maximal steady-state rates of photosynthesis were similar in plants grown at the higher CO_2 concentration, whether the leaf received adaxial or abaxial illumination (Fig. 3a(ii)). Stomatal conductance decreased

Table 1 The effects of CO₂ enrichment on plant biomass (a) and leaf parameters (b) in *Paspalum dilatatum* plants grown at either 350 or 750 µl l⁻¹ CO₂

Parameter	(a)	
	350 µl l ⁻¹ CO ₂	700 µl l ⁻¹ CO ₂
Total leaf number	112 ± 15.39 a	136 ± 23.65 b
Total leaf area (m ²)	55.38 ± 10.19 a	91.83 ± 18.76 b
Leaf dry weight (g)	1.89 ± 0.315 a	3.29 ± 0.842 b
Stem dry weight (g)	3.42 ± 0.655 a	5.37 ± 1.436 b
Root dry weight (g)	1.93 ± 0.616 a	5.37 ± 1.436 b
Total plant dry weight (g)	9.36 ± 1.913 a	18.29 ± 6.768 b
Shoot:root ratio (g g ⁻¹ DW)	1.36 ± 0.233 a	0.98 ± 0.203 b

Data represent the average ± SD for 12–14 plants at each CO₂ concentration. The different letters represent statistical differences at $P < 0.05$.

Parameter	(b)	
	350 µl l ⁻¹ CO ₂	700 µl l ⁻¹ CO ₂
SLA (m ² kg ⁻¹)	29.35 ± 1.899 a	28.34 ± 2.322 a
LAR (m ² kg ⁻¹)	5.98 ± 0.533 a	5.31 ± 0.922 a
LWR (kg kg ⁻¹)	0.20 ± 0.017 a	0.19 ± 0.026 a
Leaf density (%)	19.39 ± 0.785 a	19.11 ± 0.786 a
Leaf thickness (g m ⁻²)	176.44 ± 10.142 a	185.68 ± 10.657 b

Data represent the average ± SD for 12–14 plants at each CO₂ concentration. The different letters represent statistical differences at $P < 0.05$.

SLA, specific leaf area; LAR, leaf area ratio; LWR, leaf weight ratio.

Table 2 The effects of CO₂ enrichment on leaf pigment and protein content in *Paspalum dilatatum* plants grown at either 350 or 750 µl l⁻¹ CO₂

Parameter	350 µl l ⁻¹ CO ₂	700 µl l ⁻¹ CO ₂
Chla (mg m ⁻²)	677 ± 50.3 a	597 ± 39.5 b
Chlb (mg m ⁻²)	177 ± 14.6 a	158 ± 10.0 b
Chla + b (mg m ⁻²)	854 ± 64.1 a	755 ± 48.7 b
Carotenoids (mg m ⁻²)	135 ± 8.6 a	125 ± 6.2 b
Soluble proteins (g m ⁻²)	3604 ± 226.1 a	3571 ± 37.1 a

Data represent the mean values ± SD for eight plants at each CO₂ concentration. The different letters represent statistical differences at $P < 0.05$.

Chl, chlorophyll.

with increasing C_i and showed similar trends whether light was supplied via the adaxial or abaxial surface of the leaves. While the trends were consistent in plants from both growth CO₂ conditions (Fig. 3a(iii,iv)), the overall values were lower in plants grown in air when irradiance entered the leaf via the adaxial surface (86%; Fig. 3a(iii)).

The light-response curves for photosynthesis of plants grown at the lower CO₂ concentration were similar regardless of the orientation of the leaves towards the light (Fig. 3b(i)). Maximal photosynthetic rates were slightly lower in plants grown at the higher CO₂ concentration when the light entered the leaf via the adaxial surface, a feature not observed when the light was oriented to the abaxial surface (Fig. 3b(ii)). Stomatal conductance increased with increasing irradiance in plants grown at both CO₂ concentrations whether light was

Table 3 Effects of CO₂ enrichment on leaf epidermal structure in *Paspalum dilatatum* plants grown at either 350 µl l⁻¹ or 750 µl l⁻¹ CO₂

Parameter	350 µl l ⁻¹ CO ₂		700 µl l ⁻¹ CO ₂	
	Adaxial	Abaxial	Adaxial	Abaxial
Epidermal cell area (µm ²)	2762 ± 843 a	2704 ± 717 a	2613 ± 861 a	2585 ± 641 a
Epidermal cells (number mm ⁻²)	283 ± 39 b	294 ± 30 b	303 ± 16 b	372 ± 20 a
Stomatal area (µm ²)	743 ± 101 a	696 ± 84 b	699 ± 101 b	627 ± 88 c
Stomatal density (number mm ⁻²)	62 ± 12 a	89 ± 5 c	75 ± 7 b	104 ± 11 d
Stomatal index	18 ± 1.6 c	23.3 ± 2.1 a	19.8 ± 1.7 b c	21.8 ± 1.8 ab
Ratio of stomata (adaxial/abaxial)	0.70		0.72	

Data represent the mean values ± SD for eight plants at each CO₂ concentration. The different letters represent statistical differences at $P < 0.05$.

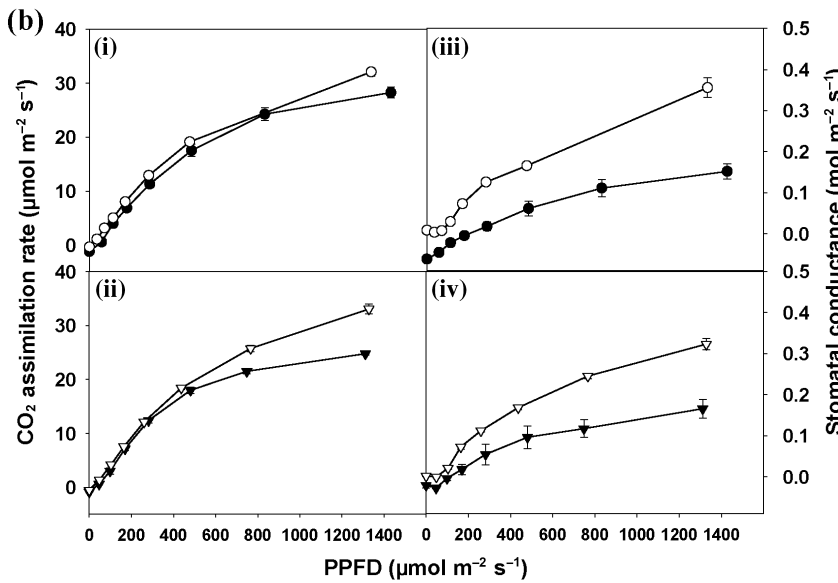
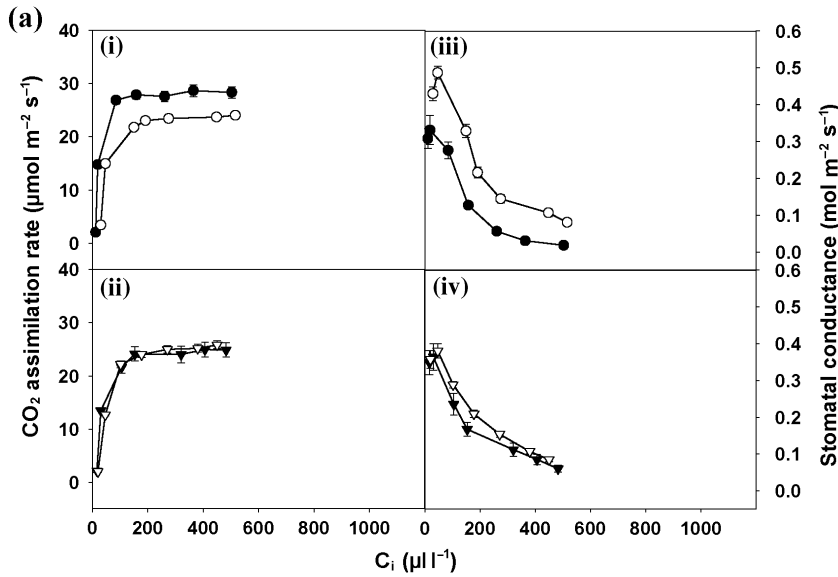


Fig. 3 The effect of light orientation on whole-leaf photosynthesis and stomatal conductance in *Paspalum dilatatum* plants that had been grown for 6 wk at either 350 $\mu\text{l l}^{-1}$ (i, iii) or 700 $\mu\text{l l}^{-1}$ CO_2 (ii, iv). (a) The CO_2 -response curves for photosynthesis (i, ii) and stomatal conductance (iii, iv) and (b) the light-response curves for whole-leaf photosynthesis (i, ii) and stomatal conductance (iii, iv) are presented. The light source was oriented either to the adaxial surface (closed circles and triangles) or to the abaxial surface (open circles and triangles). Data are the mean values \pm SE of three plants at each CO_2 concentration. PPF, photosynthetic photon flux density.

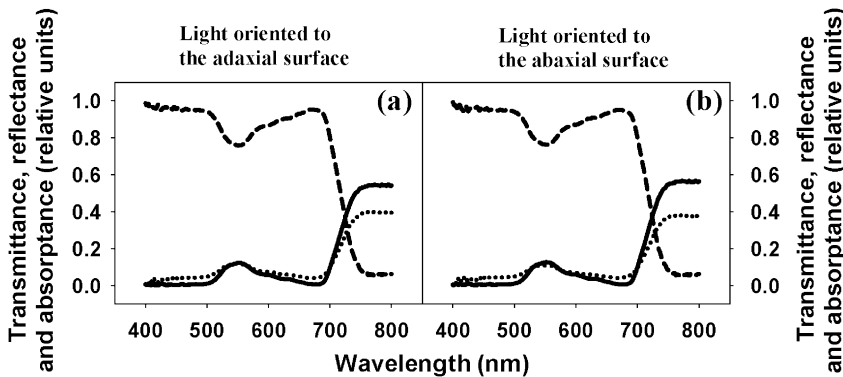


Fig. 4 The effect of light orientation on the transmittance (solid line), reflectance (dotted line) and absorbance (dashed line) spectra of *Paspalum dilatatum* leaves. Measurements were made on plants that had been grown for 6 wk at 350 $\mu\text{l l}^{-1}$ CO_2 . The light source was oriented to either (a) the adaxial surface or (b) the abaxial surface. A single representative data set is shown.

supplied via the adaxial or abaxial surface (Fig. 3b(iii,iv)). However, values were higher when the light entered the leaf via the abaxial surface (Fig. 3b(iii,iv)).

Leaf absorbance, transmittance and reflectance profiles

were similar on the adaxial and abaxial surfaces in plants grown at the lower CO_2 concentration across the light spectrum from 400 to 800 nm, whether light was supplied via the adaxial (Fig. 4a) or abaxial (Fig. 4b) surface.

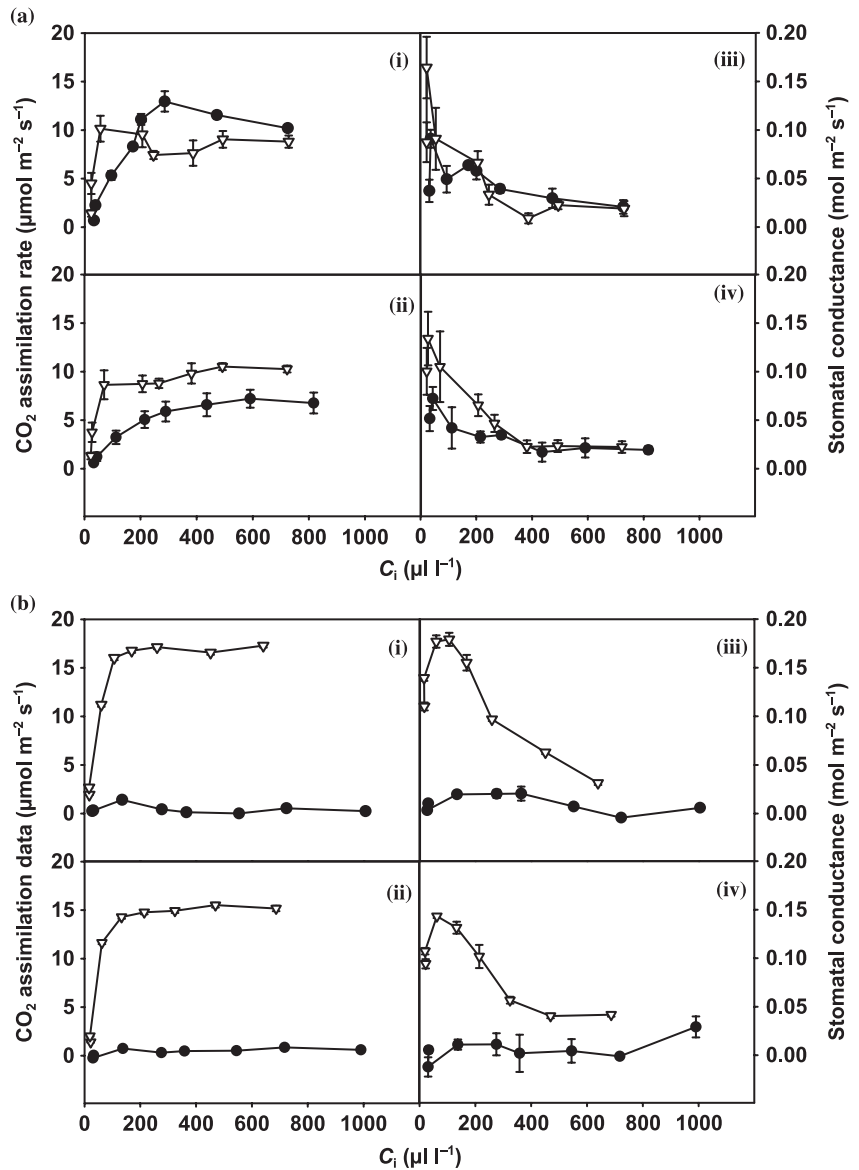


Fig. 5 The effect of light orientation on the CO₂-response curves (a, b) for photosynthetic rate (i, ii) and stomatal conductance (iii, iv) on the adaxial (closed circles) and abaxial surfaces (open triangles) of *Paspalum dilatatum* plants that had been grown for 6 wk at either 350 μl l⁻¹ CO₂ (i, iii) or 700 μl l⁻¹ CO₂ (ii, iv). The light source was oriented to either (a) the adaxial surface or (b) the abaxial surface. Data are the mean values ± SE of three plants from each CO₂ concentration.

Adaxial and abaxial photosynthesis

The adaxial surface had much lower rates of CO₂ assimilation than the abaxial leaf surface at low C_i values, regardless of the growth CO₂ concentration (Fig. 5a(i,ii),b(i,ii)). Maximal CO₂ assimilation rates in plants grown in air were similar on the two leaf surfaces when light was oriented to the adaxial surface (Fig. 5a(i)). However, when light was oriented directly to the abaxial surface, maximal photosynthesis rates were higher on this surface (Fig. 5a(ii)). In marked contrast, no CO₂ assimilation was detected on the adaxial surface under these conditions (Fig. 5a(ii)). Similar trends were observed in plants grown with CO₂ enrichment (Fig. 5b(i,ii)) except that photosynthetic rates on the abaxial surface were always higher than those on the adaxial surface when the light was oriented to the adaxial surface (Fig. 5b(i)). When light was oriented to

the adaxial surface, stomatal conductance patterns decreased with increasing C_i on both leaf surfaces (Fig. 5a(iii,iv)). When the light was oriented to the abaxial surface, higher values of stomatal conductance were found on this side of the leaf (Fig. 5b(iii,iv)). In contrast, no stomatal conductance was detected on the adaxial surface in these conditions regardless of the growth CO₂ concentration (Fig. 5b(iii,iv)).

When light was oriented to the adaxial surface, the photosynthesis rates on the two leaf surfaces increased with irradiance in a similar manner in the air-grown plants (Fig. 6a(i)). In contrast, when light was oriented to the abaxial surface, photosynthetic rates on the adaxial surface remained close to the compensation point regardless of the light intensity applied (Fig. 6b(i)). In marked contrast, the abaxial surface showed even higher CO₂ assimilation rates than when light was oriented to the adaxial surface (Fig. 6a(i),b(i)).

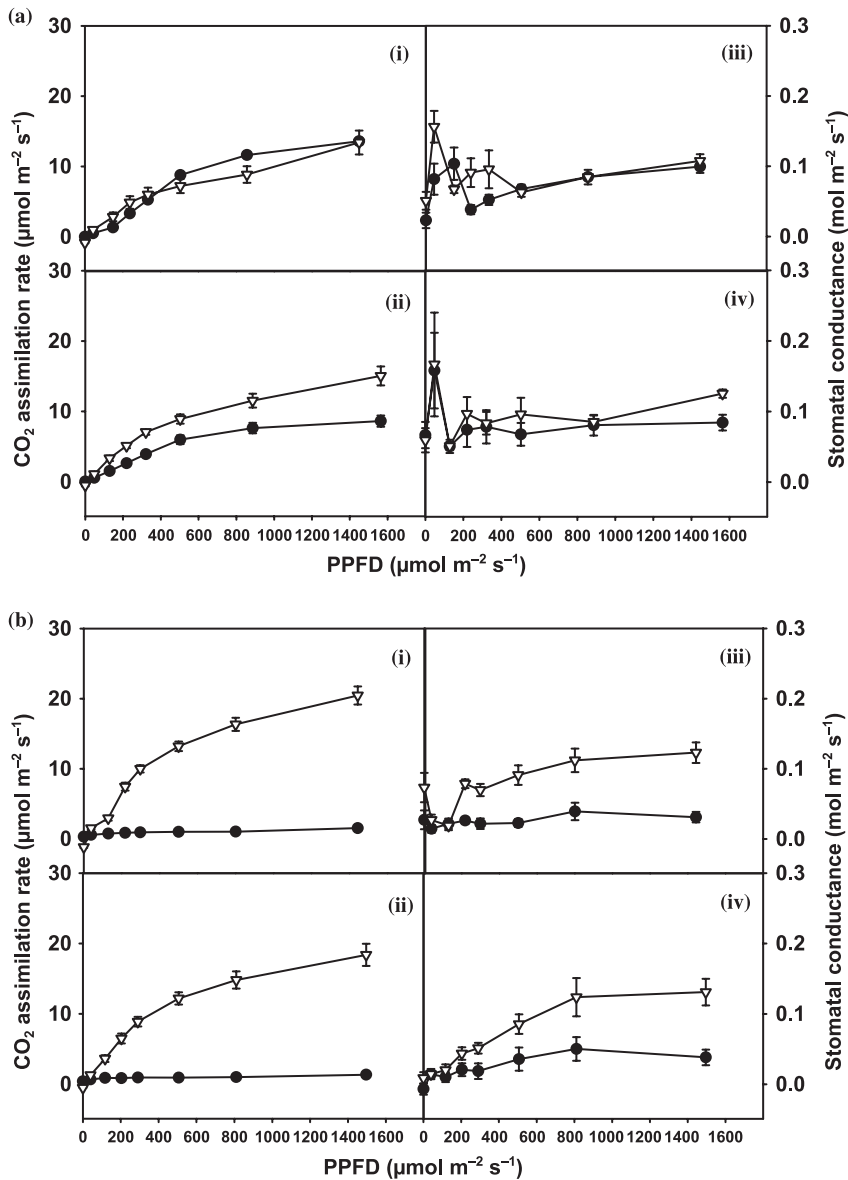


Fig. 6 The effect of light orientation on the light-response curves (a, b) for photosynthetic rate (i, ii) and stomatal conductance (iii, iv) on the adaxial (closed circles) and abaxial surfaces (open triangles) of *Paspalum dilatatum* plants that had been grown for 6 wk at either 350 $\mu\text{l l}^{-1}$ CO_2 (i, iii) or 700 $\mu\text{l l}^{-1}$ CO_2 (ii, iv). The light source was oriented to either (a) the adaxial surface or (b) the abaxial surface. Data are the mean values \pm SE of three plants from each CO_2 concentration. PPFD, photosynthetic photon flux density.

Similar trends were observed with plants grown at high CO_2 (Fig. 6a(ii),b(ii)) except that photosynthetic rates on the abaxial surface were always higher than those on the adaxial surface, independent of light orientation to the leaf. Stomatal conductance values were similar on the two leaf surfaces when light was oriented to the adaxial leaf surface, whether plants were grown in air or high CO_2 concentrations (Fig. 6a(iii,iv)). When light was oriented to the adaxial surface, stomatal conductance patterns were similar with respect to increasing light on the two leaf surfaces (Fig. 6a(iii,iv)). When the light was oriented to the abaxial surface, however, higher values of stomatal conductance were found on this side of the leaf regardless of the growth CO_2 concentration (Fig. 6a(iii,iv)). In contrast, stomatal conductance values were very low on the adaxial surface in these conditions regardless of the growth CO_2 concentration (Fig. 6b(iii,iv)).

Structure of the leaf vascular and mesophyll tissues

The air-grown *P. dilatatum* leaves have a single layer of BS cells surrounded by the M cells (Fig. 7a). The BS was composed of three to five larger cells on the adaxial side with between two and four smaller cells on the abaxial side (Fig. 7a). The relative variation in BS cell numbers was always consistent. For example, if the bottom side of the BS had four cells then the top side of the BS had three cells and if the bottom had three BS cells then the top had two BS cells. The mean value obtained for 50 different vascular bundles was 4.1 BS cells on the abaxial side and 3.0 cells on the adaxial side. The number of chloroplasts per cell ranged from three to eight in the BS and from four to seven in the M, regardless of the position in the leaf. The area occupied by chloroplast area was much higher in the BS cells ($27.9 \pm 7.5 \mu\text{m}^2$; \pm standard deviation) than in the M cells ($7.6 \pm 1.8 \mu\text{m}^2$).

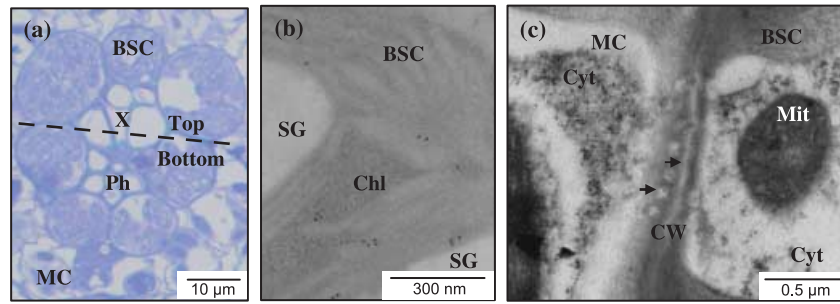


Fig. 7 (a) The structure of the *Paspalum dilatatum* vascular bundle sheath and (b) immunogold labelling of ribulose 1,5-bisphosphate carboxylase/oxygenase (Rubisco) and (c) phosphoenolpyruvate carboxylase (PEPC) proteins in the leaves of 6-wk-old *P. dilatatum* plants grown at 350 $\mu\text{l l}^{-1}$ CO_2 . BSC, bundle sheath cell; MC, mesophyll cell; X, xylem; Ph, phloem; SG, starch grain; Chl, chloroplast; Cyt, cytoplasm; CW, cell wall; Mit, mitochondria. Dashed line, plane of the leaf, indicates the zone of separation between the top and the bottom of the BS. Arrows indicate plasmodesmata.

Table 4 Quantification of immunogold labelling for ribulose 1,5-bisphosphate carboxylase/oxygenase (Rubisco) and phosphoenolpyruvate carboxylase (PEPC) proteins in the adaxial and abaxial sides of *Paspalum dilatatum* leaves

	Rubisco in the chloroplasts (gold particles μm^{-2})	PEPC in the cytosol (gold particles μm^{-2})
Bundle sheath cells		
Adaxial side	14.6 \pm 3.0 a	7.0 \pm 3.1 a
Abaxial side	15.6 \pm 3.2 a	7.5 \pm 3.5 a
Mesophyll cells		
Adaxial side	3.44 \pm 1.1 b	306 \pm 52 b
Abaxial side	3.53 \pm 1.1 b	333 \pm 50 b

Plants were grown at 350 $\mu\text{l l}^{-1}$ CO_2 .

Data represent the mean values \pm SD for 15 cells of three plants ($n = 45$). Independent analyses for Rubisco and PEPC were performed. The different letters represent statistical differences at $P < 0.05$.

In situ distribution of ribulose 1,5-bisphosphate carboxylase/oxygenase and phosphoenolpyruvate carboxylase

In situ immunolocalization studies were performed on the leaves of *P. dilatatum* plants grown at 350 $\mu\text{l l}^{-1}$ CO_2 using specific antibodies against either the Rubisco large subunit (Fig. 7b) or the PEPC protein (Fig. 7c). This analysis revealed that these enzyme proteins were uniformly distributed across the leaf. No significant differences ($P > 0.05$) in the amounts of Rubisco or PEPC proteins were found in the adaxial and abaxial cells of the BS or M tissues across the leaf blade (Table 4).

Discussion

An accurate knowledge of the impacts of the environment on photosynthesis in pasture grasses such as *P. dilatatum* is crucial in any prediction of ecosystem viability and sustainability in the face of climate change. Here we show that *P. dilatatum* plants grew better and had double the total biomass under the high CO_2 growth conditions. *Paspalum dilatatum* benefits from CO_2 enrichment in terms of growth and biomass production, as observed in other C_4 species (e.g. Ghannoum *et al.*, 1997, 2001; Wand *et al.*, 1999, 2001). These results are perhaps surprising given the widely accepted view that C_4

plants might benefit less than their C_3 counterparts from growth in a high CO_2 world because of their intrinsic CO_2 -concentrating mechanisms (Bowes, 1993). However, the presence of the ATP-dependent CO_2 -concentrating systems in C_4 species has probably already resulted in a substantial degree of acclimation of photosynthesis to a CO_2 -enriched state, at least in the BS cells. C_4 species may therefore accommodate the large increases in carbon gain that result from CO_2 enrichment better than C_3 species. In the present study, the *P. dilatatum* plants grown at the higher CO_2 concentration had decreased shoot:root ratios and showed other changes in whole-plant morphology parameters that are consistent with the acclimation of source–sink processes to CO_2 enrichment and increased carbon gain (Ghannoum *et al.*, 1997, 2001; Walting & Press, 1997).

Acclimation to CO_2 enrichment often involves changes in leaf morphology, stomatal patterning and the structure of the leaf epidermis (Lake *et al.*, 2001; Martin & Glover, 2007). Growth at the higher CO_2 concentration increased the density of stomata in *P. dilatatum* leaves, particularly on the abaxial surface, as has been reported in *Panicum antidotale* (Tipping & Murray, 1999). However, the changes observed here in *P. dilatatum* were somewhat different from those observed previously in maize, which is also a C_4 monocotyledonous NADP-malic enzyme species (Driscoll *et al.*, 2006). Maize

leaves grown with CO₂ enrichment had fewer, much larger cells on both surfaces. *Paspalum dilatatum* leaves grown under similar conditions had a greater number of smaller stomata on both surfaces with a significant increase in epidermal cell numbers only on the abaxial surface. The nature of the responses of epidermal structure to CO₂ enrichment is therefore species-specific. This is perhaps not surprising given the complex repertoire of environmental and developmental signals that influence cell size and cell number (Taylor *et al.*, 1994, 2001; Masle, 2000; Ferris *et al.*, 2001, 2002) as well as stomatal density and patterning (Larkin *et al.*, 1997; Lake *et al.*, 2002). However, stomatal densities were increased by high CO₂ in the present study with *P. dilatatum* as in *P. antidotale* (Tipping & Murray, 1999), suggesting that CO₂ is a less powerful negative regulator of stomatal density in *Paspalum* and *Panicum* than in *Arabidopsis* (Gray *et al.*, 2000).

Like maize leaves (Domes, 1971; Driscoll *et al.*, 2006), *P. dilatatum* leaves display a pronounced dorso-ventral asymmetry in the regulation of photosynthesis, each surface showing unique characteristic responses to available CO₂ and light. The specific dorso-ventral regulation of photosynthesis with respect to light orientation to the adaxial or abaxial surface was observed at both growth CO₂ concentrations. This regulation is not related to surface-dependent differences in light absorption, reflectance or transmission as the two leaf surfaces have the same optical properties. Light-harvesting complexes and photosystems are therefore equally distributed on the adaxial and abaxial sides of the leaf. While it is logical to assume that gradients in CO₂ fixation rates that have been documented in dicotyledonous C₃ leaves (Oya & Laisk, 1976; Terashima, 1986; DeLucia *et al.*, 1991; Sun & Nishio, 2001; Evans & Vogelmann, 2003) are also present in monocotyledonous C₄ leaves, there have been no comparative studies on C₄ leaves that enable deductions to be made regarding the nature of possible mechanisms of acclimation to growth at high CO₂. However, it is clear that the dorso-ventral gradients in photosynthetic machinery that determine adaxial/abaxial light absorption and CO₂ fixation characteristics in C₃ leaves must be entrained early in leaf development (Smith & Ullberg, 1989; Evans *et al.*, 1993; Poulson & DeLucia, 1993; James & Bell, 2000; Ustin *et al.*, 2001) as they can only be changed by inversion of the leaves at the onset of development (Terashima *et al.*, 1986; Smith *et al.*, 1997). Similar to the leaves of other monocotyledonous species, *P. dilatatum* leaves grow vertically from the sheath and then bend over so that the adaxial surface tends to be uppermost with the abaxial surface beneath. However, the leaves tend to curl as they expand so that the adaxial and abaxial surfaces can both experience orientation to the light in different sections of the same leaf.

The degree of stomatal opening was markedly affected by light orientation in *P. dilatatum* leaves. Abaxial illumination resulted in the closure of stomata on the adaxial surface, a response that was accompanied by a complete suppression of photosynthesis. The differential sensitivity of adaxial and

abaxial stomata to light and the absence of CO₂ transport between the two surfaces are important factors governing overall photosynthesis rates (Turner, 1970; Pospíšilová & Solárová, 1980). However, the complete suppression of photosynthesis on the adaxial surface when the stomata are closed is surprising given that this is a C₄ species able to fix CO₂ even with closed stomata, as a result of the presence of a high-affinity PEPC (Bauwe, 1986). Furthermore, these data show that there is little transfer of CO₂ across the leaf as the abaxial stomata were open in these conditions.

Photosynthesis on the adaxial surface was much less responsive to low C_i values than that on the abaxial surface. The initial slopes of the CO₂-response curves, which represent the maximal PEPC rate according to von Caemmerer (2000), indicate a higher maximal PEPC activity on the abaxial surface. The immunolocalization studies reported here show that there is a more or less uniform distribution of the carboxylating enzyme (Rubisco and PEPC) proteins across the *P. dilatatum* leaf. PEPC activation in response to increasing light intensities and other factors occurs via post-translational regulation involving an increase in the phosphorylation state of the enzyme protein (Chollet *et al.*, 1996). Our data therefore strongly suggest that dorso-ventral asymmetric gradients operate in *P. dilatatum* leaves and that these greatly affect the photosynthetic capacity on each surface. We are drawn to the conclusion that the dorso-ventral gradient in photosynthesis in *P. dilatatum* leaves results from asymmetric enzyme activation across the leaf, which allows much higher activation on the abaxial surface.

Whole-leaf photosynthesis displayed a higher degree of flexibility with regard to light orientation when the *P. dilatatum* plants were grown at the higher CO₂ concentration. The characteristic decreases in maximal CO₂ assimilation rates observed with respect to C_i when the light was oriented to the abaxial surface were absent in plants grown at the higher CO₂ concentration. Hence, CO₂ enrichment caused a small but important adjustment in the dorso-ventral specification of photosynthesis. Light absorption profiles in *Flaveria bidentis* and maize have shown that, while green light is absorbed throughout the leaf, blue light is only strongly absorbed near the surface with little light penetrating the BS cells (J.R. Evans, T.C. Vogelmann & S. von Caemmerer, pers. comm.). However, given the similarity of internal structure on the adaxial and abaxial sides of monocotyledonous leaves, which have a bilateral symmetry, one would predict that light orientation would have similar levels of penetration from each surface (Moss, 1964; Syvertsen & Cunningham, 1979). Growth at the higher CO₂ concentration had little effect on the overall photosynthetic capacity of *P. dilatatum* leaves, as observed previously (von Caemmerer *et al.*, 2001). However, other studies using CO₂ enrichment have yielded rather mixed results in different C₄ species. In some studies, enhancement of photosynthesis was reported (LeCain & Morgan, 1998; Wand *et al.*, 2001) but in others down-regulation of photosynthesis was observed (Greer *et al.*, 1995; Ghannoum *et al.*, 1997; Walting

& Press, 1997). Here we show that growth at the higher CO₂ concentration caused a small but important adjustment in the dorso-ventral specification of photosynthesis, an effect that was most apparent when light was oriented to the adaxial surface. These results indicate that metabolic and/or structural adjustments to CO₂ enrichment have occurred within the leaves and that these facilitate the altered response to light orientation.

We conclude that the dorso-ventral specification in the regulation of photosynthesis and stomatal conductance in *P. dilatatum* arises from genetically programmed differences in stomatal sensitivity to light orientation coupled to a fixed gradient in enzyme activation, probably PEPC activation state. The results presented here together with those reported previously in maize (Driscoll *et al.*, 2006) suggest that dorso-ventral asymmetry in the regulation of photosynthesis and stomatal conductance may be a common feature of monocotyledonous C₄ species. The dorso-ventral asymmetry may have functional significance in situations that favour leaf rolling, for example drought avoidance, where such mechanisms would help to prevent water deficits while allowing high rates of photosynthesis.

Acknowledgements

ASS was supported by the Fundação para a Ciência e a Tecnologia (PhD grant no. SFRH/13728/2003), the Fundação Calouste Gulbenkian and the Society for Experimental Biology. Rothamsted Research receives grant-aided support from the UK Biotechnology and Biological Sciences Research Council. The authors thank Dr G. L. Lockett, Margot Forage Germplasm Centre, New Zealand for providing the *P. dilatatum* cv. Raki seeds. We are deeply indebted to Bob Furbank and Susanne von Caemmerer for critical reading of the manuscript and also to Till Pellny for the photographs in Fig. 1.

References

- Bauwe H. 1986. An efficient method for the determination of Km values for HCO₃ of phosphoenolpyruvate. *Planta* **169**: 356–360.
- Bernardes da Silva A, Rodrigues Á, Arrabaça MC. 1999. Phosphoenolpyruvate carboxylase activity in *Paspalum dilatatum* Poir. grown at different nitrogen nutrition. *Agronomia Lusitana* **47**: 239–247.
- Bowes G. 1993. Facing the inevitable: plants and increasing atmospheric CO₂. *Annual Review of Plant Physiology and Plant Molecular Biology* **44**: 309–332.
- Bradford MM. 1976. A rapid and sensitive method for the quantification of microgram quantities of protein utilizing the principle of protein dye-binding. *Analytical Biochemistry* **72**: 248–254.
- Brown RH. 1999. Agronomic implications of C₄ photosynthesis. In: RF Sage, RK Monson, eds. *C₄ plant biology*. San Diego, CA, USA: Academic Press, 473–507.
- von Caemmerer S, Ghannoum O, Conroy JP, Clark H, Newton PCD. 2001. Photosynthetic responses of temperate species to free air CO₂ enrichment (FACE) in a grazed New Zealand pasture. *Australian Journal of Plant Physiology* **28**: 439–450.
- von Caemmerer S. 2000. Biochemical models of leaf photosynthesis. In: *Techniques in plant sciences*. Collingwood, Australia: CSIRO Publishing, 91–122.
- Carmo-Silva AE, Soares AS, Marques da Silva J, Bernardes da Silva A, Keys AJ, Arrabaça MC. 2007. Photosynthetic responses of three C₄ grasses of different metabolic subtypes to water deficit. *Functional Plant Biology* **34**: 204–213.
- Cavaco AM, Bernardes da Silva A, Arrabaça MC. 2003. Effects of long-term chilling on growth and photosynthesis of the C₄ Gramineae *Paspalum dilatatum*. *Physiologia Plantarum* **119**: 87–96.
- Chollet R, Vidal J, O'Leary MH. 1996. Phosphoenolpyruvate carboxylase: a ubiquitous, highly regulated enzyme in plants. *Annual Review of Plant Physiology and Plant Molecular Biology* **47**: 273–298.
- Coupe SA, Palmer BG, Lake JA, Overy SA, Oxborough K, Woodward FI, Gray JE, Quick WP. 2006. Systemic signalling of environmental cues in *Arabidopsis* leaves. *Journal of Experimental Botany* **57**: 329–341.
- Croxdale J. 1998. Stomatal patterning in monocotyledons: *Tradescantia* as a model system. *Journal of Experimental Botany* **49**: 279–292.
- Cui M, Vogelmann TC, Smith WK. 1991. Chlorophyll and light gradients in sun and shade leaves of *Spinacia oleracea*. *Plant, Cell & Environment* **14**: 493–500.
- DeLucia EH, Sheno HD, Naidu SL, Day TA. 1991. Photosynthetic symmetry of sun and shade leaves of different orientations. *Oecologia* **87**: 51–57.
- Domes W. 1971. Different CO₂ sensitivities of the gas exchange of the two leaf surfaces of *Zea mays*. *Planta* **98**: 186–189.
- Driscoll SP, Prins A, Olmos E, Kunert KJ, Foyer CH. 2006. Specification of adaxial and abaxial stomata, epidermal structure and photosynthesis to CO₂ enrichment in maize leaves. *Journal of Experimental Botany* **57**: 381–390.
- Evans JR. 1995. Carbon fixation profiles do reflect light absorption profiles in leaves. *Australian Journal of Plant Physiology* **22**: 865–873.
- Evans JR, Jakobsen I, Ögren E. 1993. Photosynthetic light-response curves. 2. Gradients of light absorption and photosynthetic capacity. *Planta* **189**: 191–200.
- Evans JR, Vogelmann TC. 2003. Profiles of ¹⁴C fixation through spinach leaves in relation to light absorption and photosynthetic capacity. *Plant, Cell & Environment* **26**: 547–560.
- Ferris R, Long L, Bunn SM, Robinson KM, Bradshaw HD, Rae AM, Taylor G. 2002. Leaf stomatal and epidermal cell development: Identification of putative quantitative trait loci in relation to elevated carbon dioxide concentration in poplar. *Tree Physiology* **22**: 633–640.
- Ferris R, Sabatti M, Miglietta F, Mills RF, Taylor G. 2001. Leaf area is stimulated in *Populus* by free air CO₂ enrichment (POPFACE), through increased cell expansion and production. *Plant, Cell & Environment* **24**: 305–315.
- Ghannoum O, von Caemmerer S, Barlow EWR, Conroy JP. 1997. The effect of CO₂ enrichment and irradiance on the growth, morphology and gas-exchange of a C₃ (*Panicum laxum*) and a C₄ (*Panicum antidotale*) grass. *Australian Journal of Plant Physiology* **24**: 227–237.
- Ghannoum O, von Caemmerer S, Conroy JP. 2001. Plant water use efficiency of 17 Australian NAD-ME and NADP-ME C₄ grasses at ambient and elevated CO₂ partial pressure. *Australian Journal of Plant Physiology* **28**: 1207–1217.
- Gray JE, Holroyd GH, van der Lee FM, Bahrami AR, Sijmons PC, Woodward FI, Schuch W, Hetherington AM. 2000. The HIC signalling pathway links CO₂ perception to stomatal development. *Nature* **408**: 713–716.
- Greer DH, Laing WA, Campbell BD. 1995. Photosynthetic responses of thirteen pasture species to elevated CO₂ and temperature. *Australian Journal of Plant Physiology* **22**: 713–722.
- James SA, Bell DT. 2000. Leaf orientation, light interception and stomatal conductance of *Eucalyptus globules* ssp. *globules* leaves. *Tree Physiology* **20**: 815–823.

- Lake JA, Quick WP, Beerling DJ, Woodward FI. 2001. Plant development: signals from mature to new leaves. *Nature* 411: 154–158.
- Lake JA, Woodward FI, Quick WP. 2002. Long-distance CO₂ signalling in plants. *Journal of Experimental Botany* 53: 183–193.
- Lambers H, Stuart Chapin S III, Pons TL. 1998. *Plant physiological ecology (Chapter 2: Photosynthesis, respiration, and long-distance transport)*. New York, NY, USA: Springer, 10–95.
- Larkin JC, Marks MD, Nadeau J, Sack F. 1997. Epidermal cell fate and patterning in leaves. *Plant Cell* 9: 1109–1120.
- LeCain DR, Morgan JA. 1998. Growth, gas exchange, leaf nitrogen and carbohydrate concentrations in NAD-ME and NADP-ME C₄ grasses grown in elevated CO₂. *Physiologia Plantarum* 102: 297–306.
- Lichtenhaler HK, Wellburn AR. 1983. Determination of total carotenoids and chlorophylls a and b of leaf extracts in different solvents. *Biochemistry Society Transactions* 11: 591–592.
- Marques da Silva J, Morão MA, Marques SC, Arrabaça MC. 1991. Photosynthesis of *Paspalum dilatatum* Poir. under nitrogen starvation. *Photosynthetica* 25: 583–588.
- Martin C, Glover BJ. 2007. Functional aspects of cell patterning in aerial epidermis. *Current Opinion in Plant Biology* 10: 70–82.
- Masle J. 2000. The effects of elevated CO₂ concentrations on cell division rates, growth patterns, and blade anatomy in young wheat plants are modulated by factors related to leaf position, vernalization, and genotype. *Plant Physiology* 122: 1399–1415.
- Millennium Ecosystem Assessment. 2005. *Ecosystems and human well-being: synthesis*. Washington, DC, USA: Island Press.
- Miyazawa SI, Livingston NJ, Turpin DH. 2006. Stomatal development in new leaves is related to the stomatal conductance of mature leaves in poplar (*Populus trichocarpa* × *P. deltoides*). *Journal of Experimental Botany* 57: 373–380.
- Moss DN. 1964. Optimum lighting of leaves. *Crop Science* 4: 131–136.
- Nishio JN, Sun J, Vogelmann TC. 1993. Carbon fixation gradients across spinach leaves do not follow internal light gradients. *Plant Cell* 5: 953–961.
- Novitskaya L, Trevanion S, Driscoll SD, Foyer CH, Noctor G. 2002. How does photorespiration modulate leaf amino acid contents? A dual approach through modelling and metabolite analysis. *Plant, Cell & Environment* 25: 821–836.
- Oya VM, Laisk AK. 1976. Adaptation of the photosynthesis apparatus to the light profile in the leaf. *Soviet Plant Physiology* 23: 381–386.
- Pearson CJ, Kemp H, Kirby AC, Launders TE, Mikled C. 1985. Responsiveness to seasonal temperature and nitrogen among genotypes of kikuyu, paspalum and bermuda grass pastures of coastal New South Wales. *Australian Journal of Experimental Agriculture* 25: 109–116.
- Pinto da Silva AR. 1969. Plantas novas e novas áreas para a flora de Portugal. *Agronomia Lusitana* 22: 15–23.
- Poorter H, Navas M-L. 2003. Plant growth and competition at elevated CO₂: on winners, losers and functional groups. *New Phytologist* 157: 175–198.
- Pospíšilová J, Solárová J. 1980. Environmental and biological control of diffusive conductances of adaxial and abaxial leaf epidermis. *Photosynthetica* 14: 90–127.
- Poulson ME, DeLucia EH. 1993. Photosynthetic and structural acclimation to light direction in vertical leaves of *Silphium terebinthinaceum*. *Oecologia* 95: 393–400.
- Reynolds ES. 1963. The use of lead citrate at high pH as an electron opaque stain in electron microscopy. *Journal of Cell Biology* 17: 208–212.
- Salisbury EJ. 1927. On the causes and ecological significance of stomatal frequency with special reference to woodland flora. *Philosophical Transactions of the Royal Society of London, Series B* 216: 1–65.
- Smith M, Ullberg D. 1989. Effect of leaf angle and orientation on photosynthesis and water relations in *Silphium terebinthinaceum*. *American Journal of Botany* 76: 1714–1719.
- Smith WK, Vogelmann TC, Bell DT, DeLucia EH, Shepherd KA. 1997. Leaf form and photosynthesis. *Bioscience* 47: 785–793.
- Sun J, Nishio JN. 2001. Why abaxial illumination limits photosynthetic carbon fixation in spinach leaves? *Plant and Cell Physiology* 42: 1–8.
- Sun J, Nishio JN, Vogelmann TC. 1998. Green light drives CO₂ fixation deep within leaves. *Plant and Cell Physiology* 39: 1020–1026.
- Syvrtsen JP, Cunningham GL. 1979. The effects of irradiating adaxial or abaxial leaf surface on the rate of net photosynthesis of *Perezia nana* and *Helianthus annuus*. *Photosynthetica* 13: 287–293.
- Taylor G, Ceulemans R, Ferris R, Gardner SDL, Shao BY. 2001. Increased leaf area expansion of hybrid poplar in elevated CO₂. From controlled environments to open-top chambers and to FACE. *Environmental Pollution* 115: 463–472.
- Taylor G, Ranasinghe S, Bosac C, Gardner SDL, Ferris R. 1994. Elevated CO₂ and plant growth: cellular mechanisms and responses of whole plants. *Journal of Experimental Botany* 45: 1761–1774.
- Terashima I. 1986. Dorsiventrality in photosynthetic light response curves of a leaf. *Journal of Experimental Botany* 37: 399–405.
- Terashima I, Evans JR. 1988. Effects of light and nitrogen nutrition on the organization of the photosynthetic apparatus in spinach. *Plant and Cell Physiology* 29: 143–155.
- Terashima I, Inoue Y. 1985a. Vertical gradient in photosynthetic properties of spinach chloroplasts dependent on intra-leaf light environment. *Plant and Cell Physiology* 24: 781–785.
- Terashima I, Inoue Y. 1985b. Palisade tissue chloroplasts and spongy tissue chloroplasts in spinach: biochemical and ultrastructural differences. *Plant and Cell Physiology* 26: 63–75.
- Terashima I, Saeki T. 1983. Light environment within a leaf. 1. Optical properties of paradermal sections of *Camellia* leaves with special reference to differences in the optical properties of palisade and spongy tissues. *Plant and Cell Physiology* 24: 1493–1501.
- Terashima I, Sakaguchi S, Hara N. 1986. Intra-leaf and intracellular gradients in chloroplast ultrastructure of dorsiventral leaves illuminated from the adaxial or abaxial side during their development. *Plant and Cell Physiology* 27: 1023–1031.
- Tippling C, Murray DR. 1999. Effects of elevated atmospheric CO₂ concentration on leaf anatomy and morphology in *Panicum* species representing different photosynthetic modes. *International Journal of Plant Science* 160: 1063–1073.
- Turner NC. 1970. Response of adaxial and abaxial stomata to light. *New Phytologist* 69: 647–653.
- Ustin SL, Jacquemoud S, Govaerts Y. 2001. Simulation of photon transport in a three-dimensional leaf: implications for photosynthesis. *Plant, Cell & Environment* 24: 1095–1103.
- Usuda H, Ku SB, Edwards GE. 1984. Rates of photosynthesis relative to activity of photosynthetic enzymes, chlorophyll and soluble protein content among ten C₄ species. *Australian Journal of Plant Physiology* 11: 509–517.
- Vogelmann TC. 1993. Plant tissue optics. *Annual Review of Plant Physiology and Plant Molecular Biology* 44: 233–251.
- Walting JR, Press MC. 1997. How is the relationship between the C₄ cereal *Sorghum bicolor* and the C₃ root hemi-parasites *Striga hermonthica* and *Striga asiatica* affected by elevated CO₂? *Plant, Cell & Environment* 20: 1292–1300.
- Wand SJE, Midgley GF, Jones MH, Curtis PS. 1999. Responses of wild C₄ and C₃ grass (Poaceae) species to elevated CO₂ concentration: a meta-analytic test of current theories and perceptions. *Global Change Biology* 5: 723–741.
- Wand SJE, Midgley GF, Stock WD. 2001. Growth responses to elevated CO₂ in NADP-ME, NAD-ME and PCK C₄ grasses and a C₃ grass from South Africa. *Australian Journal of Plant Physiology* 28: 13–25.
- Woodward FI, Kelly CK. 1995. The influence of CO₂ concentration on stomatal density. *New Phytologist* 131: 311–327.
- Woodward FI, Lake JA, Quick WP. 2002. Stomatal development and CO₂: Ecological consequences. *New Phytologist* 153: 477–484.